Surgical and Radiologic Anatomy (2020) 42:749–759
https://doi.org/10.1007/s00276-020-02448-0

ORIGINAL ARTICLE

Radiologic analysis of the location, shape and size of the external aperture of the carotid canal in children

Barış Ten[1] · Orhan Beger[2] · Meltem Çobanoğulları Direk[3] · Yüksel Balcı[1] · Fatih Çiçek[2] · Hakan Özalp[4] · Vural Hamzaoğlu[4] · Gülhan Temel[5] · Yusuf Vayisoğlu[6] · Celal Bağdatoğlu[4] · Derya Ümit Talas[6]

Received: 1 January 2020 / Accepted: 14 February 2020 / Published online: 27 February 2020

Abstract

Objectives This retrospective computed tomography (CT) study was aimed to assess the growth dynamic of the external aperture of the carotid canal (EACC) in children aged between 1 and 20 years.

Methods Two hundred patients (sex 100 females/100 males, average age 10.50 ± 5.77 years) with good head CT image quality were included in this study. CT images of the patients were used to obtain data related to the location, shape and dimension of EACC.

Results EACC shapes were identified as oval shaped, round shaped, and tear-drop shaped in 58.3% (233 sides), 24% (96 sides) and 17.8% (71 sides), respectively. EACC length, disEACC–MSP (distance between EACC and midsagittal plane), and EACC width did not change from the prepubescence period; while, the disEACC–SC (distance between EACC and supramastoid crest) seemed to reach adult size in the postpubescence period. Linear functions for EACC length and width were calculated as: $y = 5.453 + 0.091 \times$ years, and $y = 5.398 + 0.059 \times$ years, respectively.

Conclusion The regression equations of the measured parameters representing the growth dynamic of EACC in children can be helpful to estimate its size, location and angulation, which suggest that the dimension and distances to certain anatomical landmarks seemed to reach adult size in different developmental periods. In this context, the findings of this study may seem to emphasize the importance of preoperative radiological evaluation on skull base, related to EACC, for multidisciplinary surgeon teams during childhood surgeries in terms of patients' positioning, and the selection of appropriate surgical approach.

Keywords Carotid canal · Childhood · Computed tomography · Morphometry · Skull base

Introduction

The craniocervical junction is a transition zone for some vital neurovascular structures (e.g., the internal carotid artery, accessory nerve, vagus nerve, middle meningeal artery, internal jugular vein, hypoglossal nerve, facial nerve, and glossopharyngeal nerve). In this complex region, the external aperture of the carotid canal (EACC) located on the lower surface of the petrous portion of the temporal bone is a entry opening from neck to head for the internal carotid artery [1, 2, 6, 7, 14, 18]. EACC morphology is important for multidisciplinary surgeon teams to avoid iatrogenic injury of the internal carotid artery or neurovascular structures passing through adjacent foramina (e.g., jugular foramen) during the treatment of pathologies (aneurysms, tumors, fractures, agenesis, stenosis etc.), and to select the appropriate surgical applications (e.g., lateral surgical approaches) due to the fact that EACC is the most easily monitored landmark

✉ Orhan Beger
obeger@gmail.com

1 Faculty of Medicine, Department of Radiology, Mersin University, Mersin, Turkey

2 Faculty of Medicine, Department of Anatomy, Mersin University, Ciftlikkoy Campus, 33343 Mersin, Turkey

3 Faculty of Medicine, Department of Pediatrics, Mersin University, Mersin, Turkey

4 Faculty of Medicine, Department of Neurosurgery, Mersin University, Mersin, Turkey

5 Faculty of Medicine, Department of Biostatistics, Mersin University, Mersin, Turkey

6 Faculty of Medicine, Department of Otorhinolaryngology, Mersin University, Mersin, Turkey

with magnetic resonance tomography angiography or digital substraction angiography [3–6, 8, 12, 15–17, 19, 21, 25]. In this context, many radioanatomic studies have been carried out on the anatomical features of EACC including its location, shape and size in the last few decades [1, 5, 6, 16, 19, 21, 26].

The studies that contain measurements between important foramina (e.g., jugular foramen), morphologic descriptions (e.g., shape), and examination of different surgical approaches (e.g., infratemporal fossa approach or lateral supracondylar approach) enrich the knowledge pool related to EACC in the literature [3–5, 8, 9, 16, 20, 22, 24, 26]; however, the information is mostly based on data from adult dry skulls [1, 2, 5, 14, 16, 18, 19, 21]. Pediatric and adult individuals show differences in some aspects such as (a) anatomical properties of the skull base, (b) the type and biological behaviors of pathological lesions (e.g., tumors), and (c) treatment procedures (e.g., the selection of appropriate surgical approaches) [9, 20, 22, 24]. Therefore, a detailed anatomical information related to EACC in children may be useful for otologists, neuroradiologists and neurosurgeons to understand the characteristics between different age periods. In this regard, the main objective of this retrospective computed tomography (CT) study conducted on children aged from one to 20 years was to examine the gross anatomy of EACC and to determine the probable changes in its location, shape and size dependent on growth.

Materials and methods

As a result of CT scans of 4592 patients (1733 females and 2859 males) admitted to Mersin University Training and Research Hospital with different complaints (e.g., headache, falling from high, traffic accident, and trauma) between January and December 2019, 200 patients (100 females and 100 males) with good head CT image quality were included in this study. The selected patients did not have any malformations (e.g., genetic or syndromic), traumatic (e.g., fracture) and pathologic etiologies (oncologic, infectious, vascular, etc.) in the skull base, especially in the temporal bones. The study was approved by the Clinical Research Ethics Committee of Mersin University (2019/553). After the scannings performed by a radiologist (B.T.) with a 64-slice scanner (Aquillion 64, 0.5-mm-thick slices, 0.3-mm interval, FOV: 240 mm, matrix: 512×512, pixel size: 0.46 mm, 230 mA, 120 kV, Toshiba Medical Systems Tokyo, Japan), the raw data were reformatted in different planes (e.g., axial, coronal and sagittal). The obtained images were used to create the three-dimensional multiplanar reconstruction (3D-MPR) views on a work station (Vitrea 2). The parameters were determined as follows (Figs. 1, 2, 3).

- The detection of EACC shape,
- EACC length (antero-posterior diameter, at the farthest level)
- EACC width (medio-lateral diameter, at the widest level),

Fig. 1 The photographs show EACC in different planes (axial, coronal an sagittal planes)

Fig. 2 The photograph shows the parameters: (**a**) EACC length, (**b**) EACC width, (**c**) disEACC–MSP, (**d**) disEACC–SC, (**e**) angZR–EACC–SC, and (**f**) angEAC–EACC–SC

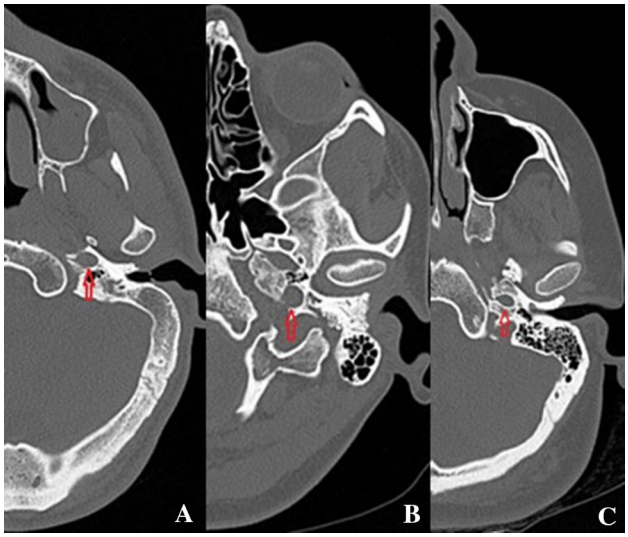

Fig. 3 The photographs show the shape of EACC. **a** oval shaped, (**b**) round shaped, and (**c**) tear-drop shaped

- The distance (disEACC–SC) between EACC and the supramastoid crest (the nearest distance),
- The distance (disEACC–MSP) between EACC and the midsagittal plane (the nearest distance),
- The angle (angZR–EACC–SC) between the zygoma root, EACC and the supramastoid crest,
- The angle (angEAC–EACC–SC) between the external acoustic porous, EACC and the supramastoid crest.

The controls of the normality and variance homogeneity were performed with Shapiro–Wilk and Levene tests, respectively. Change in the measurements related to EACC dependent on growth (between 1 and 20 years) was examined by one-way ANOVA and post hoc Bonferroni test. In addition, considering the growth periods in childhood including infancy (between 0 and 2 years), early childhood (between 3 and 5 years), later childhood (between 6 and 9 years), prepubescence (between 10 and 13 years), and postpubescence (between 14 and 20 years) periods [11], the parameters belonging to the age groups were compared with one-way ANOVA and post hoc Bonferroni test. Those tests were also used to compare the measured parameters according to EACC shape. The sides (the paired-sample *t* test) and sexes (the independent-sample *t* test) analyses were performed with Student's *t* test. Moreover, the paired sample *t* test was used to compare the diameters (length and width), distances (disEACC–SC and disEACC–MSP), or angles (angZR–EACC–SC and angEAC–EACC–SC). The correlations between the measured parameters were assessed with the Pearson correlation coefficient test. Chi-square test was utilized for the assessment of relation between EACC shapes and the age groups. The simple linear regression and the calculated regression equations were used to show the alteration in the measured parameters related to EACC dependent on growth (between 1 and 20 years). The threshold for statistical significance was set as $p < 0.05$.

Results

In the study, CT images of 200 patients aged from 1 to 20 years (at mean 10.50 ± 5.77 years) were used, 10 (5 females and 5 males) patients for each age (Table 1). The findings of this study were summarized as follows:

- The measurements showed that the disEACC–SC, EACC length, disEACC–MSP, and EACC width according to age between 1 and 20 years were increasing; while the angZR–EACC–SC was decreasing ($p < 0.001$). The angEAC–EACC–SC showed an irregular pattern (Table 1).
- The disEACC–MSP, EACC width and length did not change from the prepubescence period. The angEAC–EACC–SC showed irregular changes between age groups. The growth of the disEACC–SC and angZR–EACC–SC were determined to be independent of age groups (Table 2).
- EACC shapes were identified as oval shaped, round shaped, and tear-drop shaped in 58.3% (233 sides), 24% (96 sides) and 17.8% (71 sides), respectively (Fig. 4).
- The distribution order of the incidence of EACC shapes in terms of males and females was found as follows: the oval shaped (127 sides, 63.5% for males and 106 sides, 53% for females) > round shaped (39 sides, 19.5% for males and 57 sides, 28.5% for females) > tear-drop shaped (34 sides, 17% for males and 37 sides, 18.5% for females) (Fig. 5).

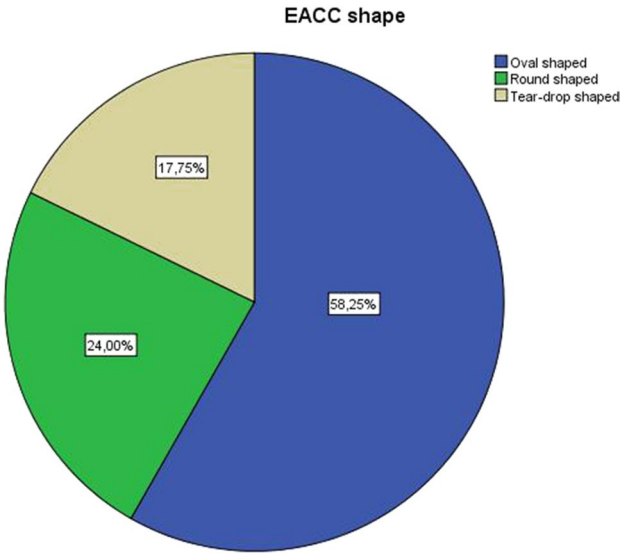

Fig. 4 The chart shows the distribution percentage of EACC shapes

- The distribution order of the incidence of EACC shapes in terms of right and left sides was found as follows: the oval shaped (112 sides, 56% for right and 121 sides, 60.5% for left) > round shaped (54 sides, 27% for right and 42 sides, 21% for left) > tear-drop shaped (34 sides, 17% for right and 37 sides, 18.5% for left) (Fig. 6).
- The measurements showed that the parameters apart from the disEACC–MSP ($p=0.391$), EACC width ($p=0.217$) and angEAC–EACC–SC ($p=0.121$) were changing according to EACC shapes (Table 3).
- The average values of the disEACC–MSP ($p=0.012$), EACC width ($p=0.026$) and EACC length ($p<0.001$) in males were significantly greater than that in females; while the mean value of the angEAC–EACC–SC ($p=0.007$) in males was smaller than that in females. The other parameters did not show significant differences in terms of sex (Table 4).
- The average values of the angEAC–EACC–SC ($p<0.001$) and EACC length ($p=0.014$) in right sides were significantly greater than that in left sides; while the mean value of the angZR–EACC–SC ($p=0.009$) in right sides was smaller than that in left sides. The other parameters did not show significant differences in terms of side (Table 4).
- Positive correlation was observed between the parameters as follows: (a) EACC length and width ($p<0.001$, $r=0.480$), (b) EACC length and disEACC–MSP ($p<0.001$, $r=0.306$), (c) EACC length and disEACC–SC ($p=0.001$, $r=0.474$), (d) disEACC–MSP and disEACC–SC ($p<0.001$, $r=0.470$), (e) EACC width and disEACC–MSP ($p<0.001$, $r=0.317$), and (f) EACC width and disEACC–SC ($p<0.001$, $r=0.326$) (Table 5).
- Negative correlation was found between the parameters as follows: (a) EACC length and angZR–EACC–SC ($p<0.001$, $r=0.318$), (b) angZR–EACC–SC and angEAC–EACC–SC ($p<0.001$, $r=0.236$), (c) angZR–EACC–SC and disEACC–SC ($p<0.001$, $r=0.614$), (d) disEACC–MSP and angEAC–EACC–SC ($p=0.037$, $r=0.104$), (e) EACC width and angZR–EACC–SC ($p<0.001$, $r=0.182$), and (f) EACC width and angEAC–EACC–SC ($p<0.001$, $r=0.167$) (Table 5).
- The spread of the incidence of EACC shapes according to age groups was given in Table 6, which showed that

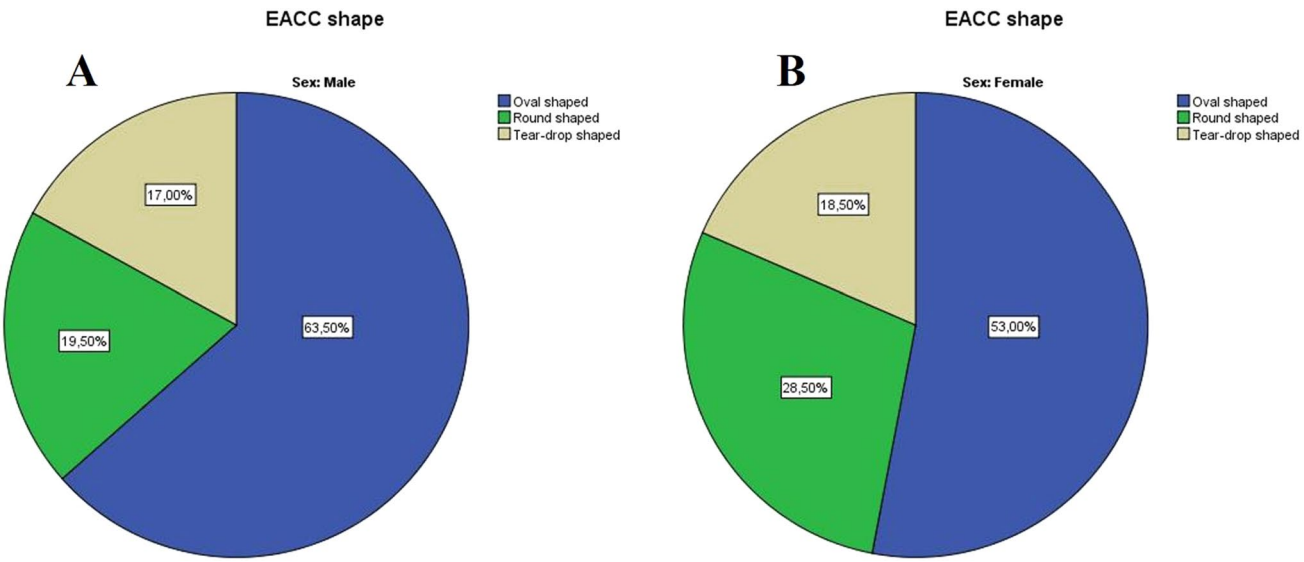

Fig. 5 The charts show the distribution percentage of EACC shapes (**a**) in males, and (**b**) in females

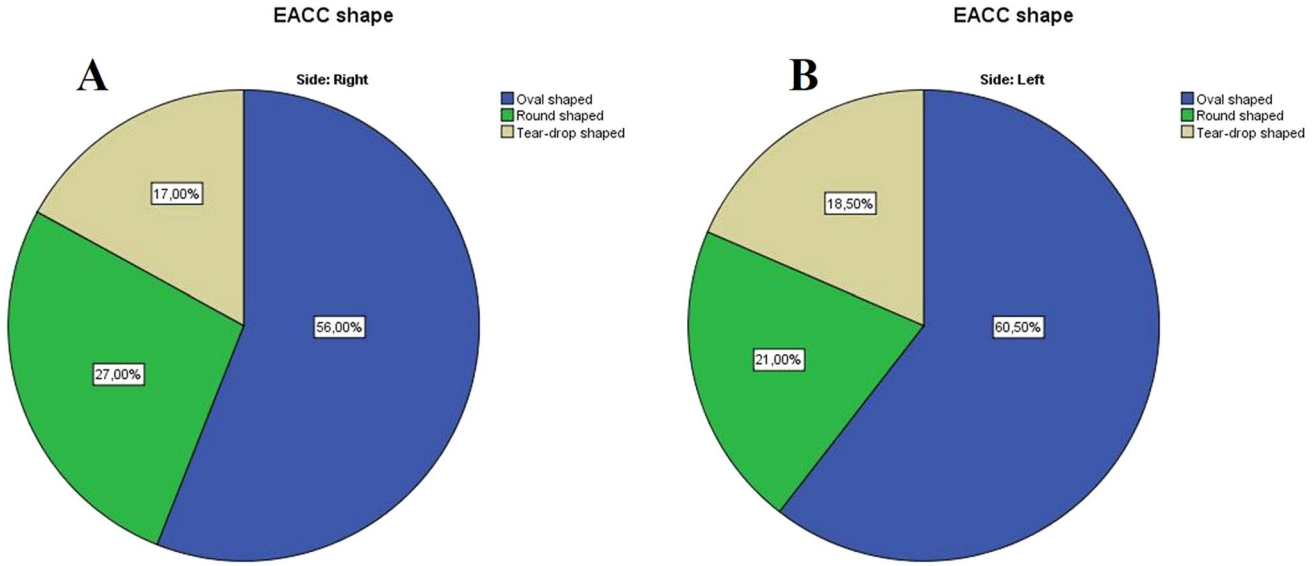

Fig. 6 The charts show the distribution percentage of EACC shapes (**a**) in right sides, and (**b**) in left sides

the shapes were not affected by age periods in children ($p = 0.084$).

- EACC length (6.41 ± 1.07) was greater than EACC width (6.01 ± 0.87) ($p < 0.001$).
- The angZR–EACC–SC (27.72 ± 5.43) was greater than the angEAC–EACC–SC (21.68 ± 4.18) ($p < 0.001$).
- The disEACC–SC (25.44 ± 4.44) was greater than the disEACC–MSP (23.80 ± 2.79) ($p < 0.001$).
- Linear functions for EACC length and width were calculated as: $y = 5.453 + 0.091 \times$ years, and $y = 5.398 + 0.059 \times$ years, respectively (Fig. 7).
- Linear functions for the angZR–EACC–SC and angEAC–EACC–SC were calculated as: $y = 32.339 - 0.439 \times$ years, and $y = 22.937 - 0.119 \times$ years, respectively (Fig. 8).
- Linear functions for the disEACC–SC and disEACC–MSP were calculated as: $y = 18.553 + 0.656 \times$ years, and $y = 20.500 + 0.314 \times$ years, respectively (Fig. 9).

Discussion

The disEACC–MSP, EACC width and length did not change from the prepubescence period; while, the disEACC–SC seemed to reach adult size in postpubescence period, which proved that EACC dimension and its distances to certain anatomical landmarks seemed to reach adult size in different

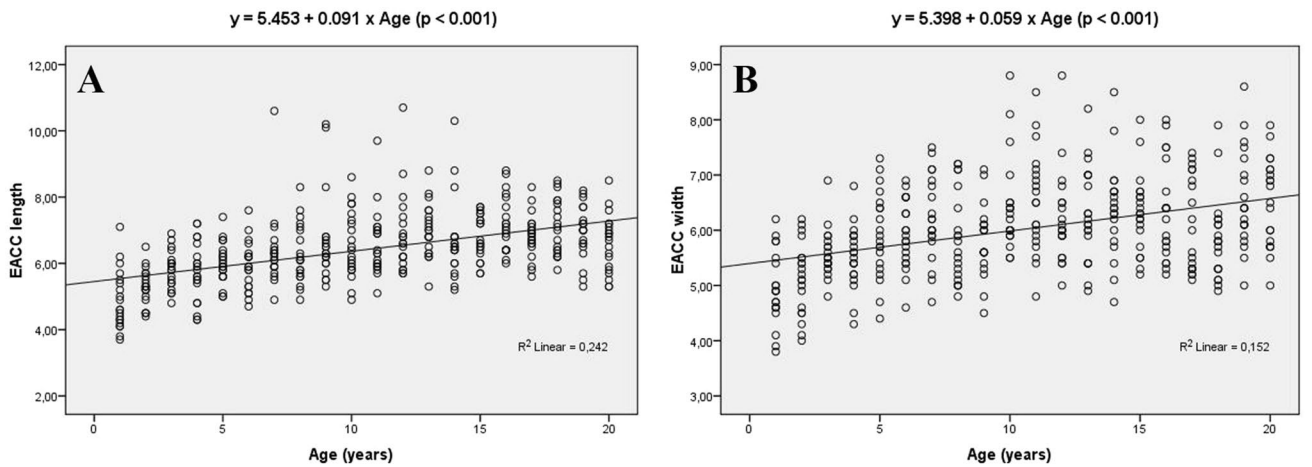

Fig. 7 The charts show the linear regression line for (**a**) EACC length, and (**b**) EACC width

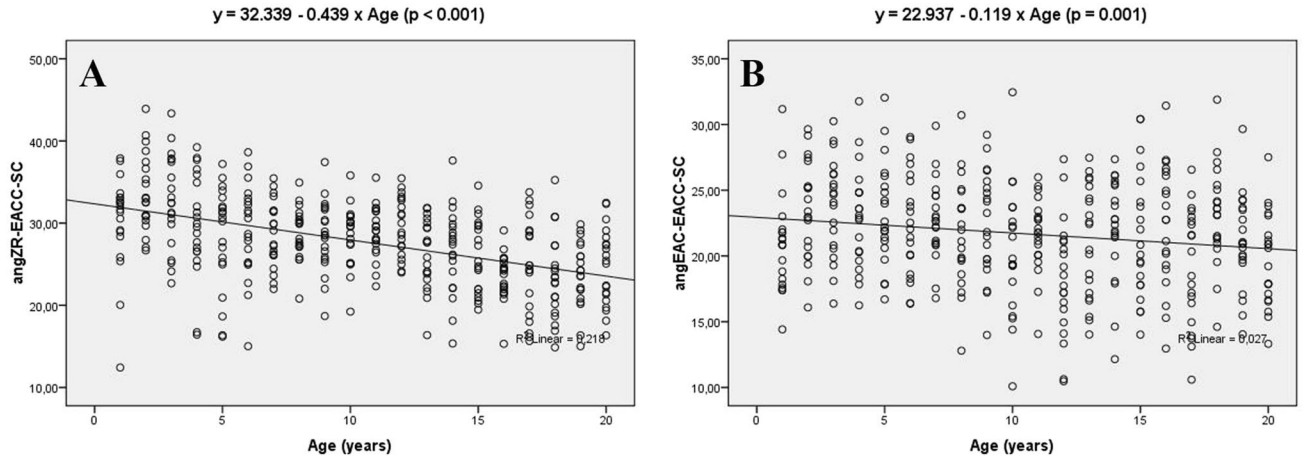

Fig. 8 The charts show the linear regression line for (**a**) angZR–EACC–SC, and B) angEAC–EACC–SC

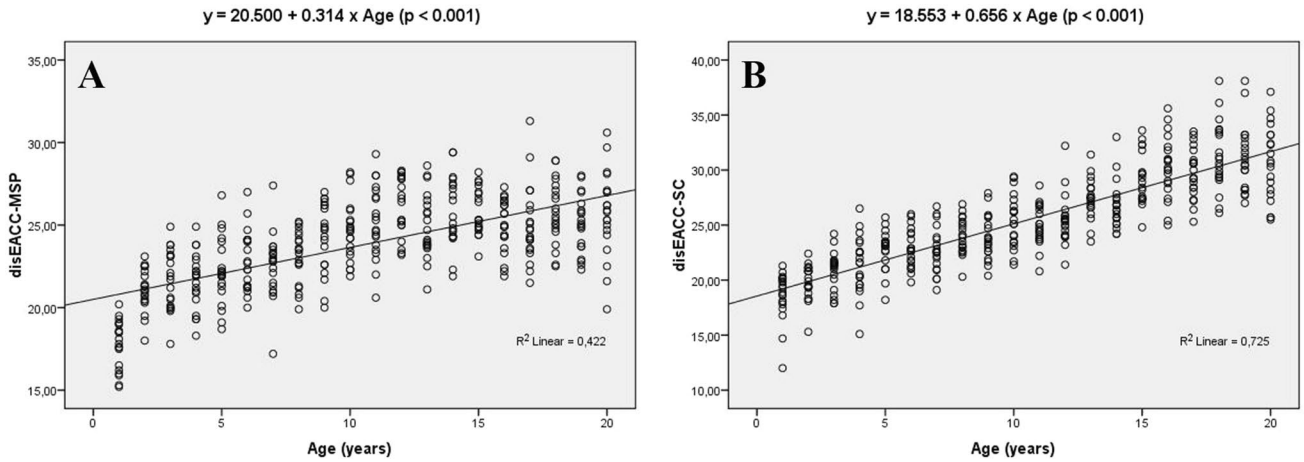

Fig. 9 The charts show the linear regression line for (**a**) disEACC–MSP, and (**b**) disEACC–SC

developmental periods. In addition, the mean of EACC length and width was found to be greater in males compared to females. These findings proved the importance of preoperative radiological evaluation in children during surgical planning.

The morphology of EACC is important for radiologists, otologists and neurosurgeons in terms of the associated abnormalities and pathologies such as carotid sympathetic plexus schwannomas, moyamoya disease, Crouzon syndrome, carotid canal fractures dependent on trauma, aneurysms, and congenital malformations (e.g., agenesis and stenosis) [12, 13, 15, 17, 23, 25, 26]. For example, EACC in the patients with Crouzon syndrome may be closer to the anatomical landmarks (e.g., midsagittal plane or foramen ovale) than normal subjects [13]. Watanabe et al. [23] found that the carotid canal diameter in patients with moyamoya disease was smaller compared to normal patients. Some pathologic conditions such as aneurysms or tumors can distort osseous structures [10]. Therefore, the normal anatomical knowledge including distance and angulation with certain anatomical landmarks may be helpful to follow the correct route in the operation area, to avoid iatrogenic injuries or complications during surgeries, and to assess effectively abnormal location, shape and dimensions in patients with malformations. In this regard, the normal anatomy of EACC has been largely examined for multidisciplinary surgeon teams in the last few decades [1, 5, 6, 14, 16, 19, 21, 26]. However, the current English literature showed that the data related to EACC were largely based on the studies performed in adult dry skulls or patients. Taking into account the children with all those pathologies and abnormalities, we think that a new dataset including shape analysis, location detection, and dimension assessment

Table 1 The measurements of the parameters related to EACC

Age (years)	Sex	N	EACC length (mm)	EACC width (mm)	disEACC–MSP (mm)	disEACC–SC (mm)	angZR–EACC–SC (°)	angEAC–EACC–SC (°)
1	5M/5F	20	4.88 ± 0.88	4.94 ± 0.65	17.77 ± 1.47	18.61 ± 2.18	30.24 ± 5.92	20.93 ± 3.79
2	5M/5F	20	5.28 ± 0.55	5.13 ± 0.65	21.06 ± 1.25	19.85 ± 1.59	33.64 ± 4.73	23.42 ± 3.75
3	5M/5F	20	5.81 ± 0.55	5.57 ± 0.43	21.68 ± 1.82	20.84 ± 1.74	32.53 ± 5.69	23.72 ± 3.72
4	5M/5F	20	5.73 ± 0.90	5.52 ± 0.56	21.64 ± 1.69	21.34 ± 2.64	29.78 ± 6.34	22.86 ± 3.87
5	5M/5F	20	6.01 ± 0.62	5.91 ± 0.78	22.22 ± 2.05	22.79 ± 1.75	28.22 ± 6.25	23.21 ± 3.96
6	5M/5F	20	5.91 ± 0.73	5.91 ± 0.61	22.78 ± 1.83	22.86 ± 1.76	29.08 ± 5.70	22.51 ± 3.98
7	5M/5F	20	6.38 ± 1.12	6.21 ± 0.76	22.56 ± 1.96	22.71 ± 2.04	28.62 ± 4.00	22.74 ± 3.05
8	5M/5F	20	6.30 ± 0.89	5.86 ± 0.82	23.04 ± 1.57	23.99 ± 1.61	28.77 ± 3.15	21.68 ± 4.12
9	5M/5F	20	6.68 ± 1.34	5.81 ± 0.64	24.30 ± 2.11	23.86 ± 1.98	28.39 ± 4.33	22.42 ± 4.02
10	5 M/5F	20	6.61 ± 1.01	6.43 ± 0.85	24.66 ± 1.85	25.38 ± 2.40	28.27 ± 3.69	20.30 ± 4.90
11	5M/5F	20	6.63 ± 1.00	6.50 ± 0.91	25.18 ± 2.20	24.94 ± 1.83	28.88 ± 3.17	21.59 ± 2.84
12	5M/5F	20	6.87 ± 1.20	6.20 ± 0.83	26.15 ± 1.78	25.46 ± 2.23	29.55 ± 3.59	18.32 ± 4.49
13	5M/5F	20	7.01 ± 0.79	6.28 ± 0.85	24.95 ± 1.96	27.37 ± 1.82	26.22 ± 4.20	21.00 ± 4.28
14	5M/5F	20	6.67 ± 1.20	6.38 ± 0.85	25.79 ± 2.10	26.73 ± 2.13	26.64 ± 5.19	22.07 ± 3.95
15	5M/5F	20	6.80 ± 0.66	6.31 ± 0.70	25.76 ± 1.36	29.14 ± 2.34	25.83 ± 4.48	21.51 ± 4.88
16	5 M/5F	20	7.16 ± 0.85	6.34 ± 0.88	24.93 ± 1.61	30.23 ± 2.83	23.46 ± 2.86	22.32 ± 4.70
17	5M/5F	20	6.82 ± 0.66	6.08 ± 0.85	24.99 ± 2.33	29.74 ± 2.30	24.67 ± 5.82	19.14 ± 4.45
18	5M/5F	20	7.09 ± 0.84	5.84 ± 0.75	25.79 ± 1.90	31.24 ± 3.10	23.32 ± 5.10	23.14 ± 3.81
19	5M/5F	20	6.94 ± 0.81	6.55 ± 0.88	25.03 ± 1.72	31.03 ± 2.94	23.70 ± 4.00	21.04 ± 3.61
20	5M/5F	20	6.61 ± 0.86	6.51 ± 0.80	25.70 ± 2.58	30.70 ± 3.39	24.62 ± 4.70	19.72 ± 3.56
10.50 ± 5.77	100M/100F	400	6.41 ± 1.07	6.01 ± 0.87	23.80 ± 2.79	25.44 ± 4.44	27.72 ± 5.43	21.68 ± 4.18
p	< 0.001	< 0.001	< 0.001	< 0.001	< 0.001	< 0.001		

M Male, *F* Female, *SC* upramastoid crest, *MSP* Midsagittal plane, *ZR* Zygoma root, External acoustic porous, dis: distance, *ang* angle, *N* Number of sides

Table 2 Comparison of the parameters according to age groups

Parameters	Infancy (*N* = 40)	Early childhood (*N* = 60)	Later childhood (*N* = 80)	Prepubescence (*N* = 80)	Postpubescence (*N* = 140)	p
EACC length (mm)	5.08 ± 0.75[b, c, d, e]	5.85 ± 0.70[a, c, d, e]	6.32 ± 1.06[a, b, d, e]	6.78 ± 1.01[a, b, c]	6.87 ± 0.86[a, b, c]	< 0.001
EACC width (mm)	5.03 ± 0.65[b, c, d, e]	5.66 ± 0.62[a, c, d, e]	5.95 ± 0.72[a, d, e]	6.35 ± 0.85[a, b, c]	6.28 ± 0.83[a, b, c]	< 0.001
disEACC–MSP (mm)	19.41 ± 2.14[b, c, d, e]	21.85 ± 1.84[a, c, d, e]	23.17 ± 1.96[a, b, d, e]	25.23 ± 2.00[a, b, c]	25.43 ± 1.98[a, b, c]	< 0.001
disEACC–SC (mm)	19.23 ± 1.99[b, c, d, e]	21.66 ± 2.21[a, c, d, e]	23.35 ± 1.91[a, b, d, e]	25.79 ± 2.25[a, b, c, e]	29.83 ± 3.05[a, b, c, d]	< 0.001
angZR–EACC–SC (°)	31.94 ± 5.56[c, d, e]	30.18 ± 6.26[e]	28.71 ± 4.32[a, e]	28.23 ± 3.82[a, e]	24.61 ± 4.72 [a, b, c, d]	< 0.001
angEAC–EACC–SC (°)	22.18 ± 3.93	23.26 ± 3.80[d]	22.34 ± 3.76[d]	20.30 ± 4.30[b, c]	21.28 ± 4.29	< 0.001

SC Supramastoid crest, *MSP* Midsagittal plane, *ZR* Zygoma root, External acoustic porous, *dis* distance, *ang* angle

[a]Comparison to infancy

[b]Comparison to early childhood

[c]Comparison to later childhood

[d]Comparison to prepubescence

[e]Comparison to postpubescence, $p < 0.05$

can enrich the information pool related to EACC and may be useful for surgeons to understand the changes in its morphology from birth to adult life.

The shapes of EACC were identified as oval shaped (58.3%, 233 sides), round shaped (24%, 96 sides), and teardrop shaped (17.8%, 71 sides) in this study. Aoun et al. [2]

Table 3 Comparison of the parameters according to EACC shape

Parameters	Oval shaped ($N=233$)	Round shaped ($N=96$)	Tear-drop shaped ($N=71$)	p
EACC length (mm)	6.47 ± 1.15^{b}	$6.10 \pm 0.80^{a, c}$	6.62 ± 1.03^{b}	0.003
EACC width (mm)	6.05 ± 0.92	5.88 ± 0.74	6.06 ± 0.81	0.217
disEACC–MSP (mm)	23.63 ± 2.80	24.01 ± 3.01	24.04 ± 2.44	0.391
disEACC–SC (mm)	25.04 ± 4.40^{c}	24.85 ± 4.03^{c}	$27.54 \pm 4.57^{a, b}$	< 0.001
angZR–EACC–SC (°)	27.96 ± 5.52^{c}	28.62 ± 4.75^{c}	$25.71 \pm 5.59^{a, b}$	0.002
angEAC–EACC–SC (°)	21.51 ± 4.14	22.42 ± 4.35	21.23 ± 3.98	0.121

SC Supramastoid crest, *MSP* Midsagittal plane, *ZR* Zygoma root, External acoustic porous, *dis* distance, *ang* angle

[a]Comparison to oval shaped

[b]Comparison to round shaped

[c]Comparison to tear-drop shaped, $p < 0.05$

Table 4 Comparison of the parameters in terms of sex and side

Parameters	Male	Female	*p*	Right	Left	p
EACC length (mm)	6.61 ± 1.12	6.20 ± 0.97	< 0.001	6.54 ± 1.07	6.27 ± 1.05	0.014
EACC width (mm)	6.11 ± 0.93	5.92 ± 0.79	0.026	6.00 ± 0.90	6.03 ± 0.84	0.705
disEACC–MSP (mm)	24.15 ± 2.83	23.45 ± 2.71	0.012	23.76 ± 2.78	23.83 ± 2.81	0.800
disEACC–SC (mm)	25.87 ± 4.81	25.01 ± 4.01	0.053	25.59 ± 4.59	25.29 ± 4.30	0.505
angZR–EACC–SC (°)	27.99 ± 5.42	27.46 ± 5.45	0.329	27.02 ± 5.52	28.43 ± 5.26	0.009
angEAC–EACC–SC (°)	21.12 ± 4.20	22.24 ± 4.08	0.007	22.99 ± 4.07	20.37 ± 3.87	< 0.001

SC Supramastoid crest, *MSP* Midsagittal plane, *ZR* Zygoma root, External acoustic porous, *dis* distance, *ang* angle

Table 5 The correlations between the parameters

Parameters	EACC width (mm)	angZR–EACC–SC (°)	angEAC–EACC–SC (°)	disEACC–MSP (mm)	disEACC–SC (mm)
EACC length (mm)	0.480^{**}	-0.318^{**}	0.003	0.306^{**}	0.474^{**}
	< 0.001	< 0.001	0.955	< 0.001	< 0.001
EACC width (mm)		-0.182^{**}	-0.167^{**}	0.317^{**}	0.326^{**}
		< 0.001	0.001	< 0.001	< 0.001
angZR–EACC–SC (°)			-0.236^{**}	−0.093	-0.614^{**}
			< 0.001	0.063	< 0.001
angEAC–EACC–SC (°)				-0.104^{*}	−0.080
				0.037	0.109
disEACC–MSP (mm)					0.470^{**}
					< 0.001

dis distance, *ang* angle

*Correlation is significant at the 0.05 level (two tailed)

**Correlation is significant at the 0.01 level (two tailed)

Table 6 Statistical evaluation of EACC shape according to age groups

Parameters	Infancy	Early chilhood	Later childhood	Prepubescence	Postpubescence	Total	*p*
Oval shaped	27 (67.5%)	37 (61.7%)	49 (61.3%)	41 (51.3%)	79 (56.4%)	233 (58.3%)	0.084
Round shaped	11 (27.5%)	17 (28.3%)	19 (23.8%)	22 (27.5%)	27 (19.3%)	96 (24%)	
Tear-drop shaped	2 (5%)	6 (10%)	12 (15%)	17 (21.3%)	34 (24.3%)	71 (17.8%)	
Total	40	60	80	80	140	400	

identified the form of EACC as oval shaped or round shaped without giving a numerical data. The percentage of the incidence of EACC shapes was given in Table 7 [14, 16, 21], where the percentage range was presented as 30.67–49.4% for oval shaped, 28.4–62.5% for round shaped, and 5–22.2% for tear-drop shaped. Unlike the studies of Özalp et al. [16] and Somesh et al. [21], the oval-shaped rate in this study was higher than round-shaped rate similar to the rate reported by Naidoo et al. [14]. On the top of it, we observed that the spread of the incidence of EACC shapes according to age groups was not affected by age periods (infancy, early childhood, later childhood, prepubescence, and postpubescence periods) in children. We also found that the distribution order of the incidence of EACC shapes in terms of sex and side was the oval shaped > round shaped > tear-drop shaped; thus, this finding proved that the incidence was not affected by sex or side. Considering Özalp et al. [16]'s study performed in Turkey, the regional differences did not probably affect the distribution order of the incidence of EACC shapes. Therefore, studies conducted on different populations and sample groups (patients, dry skulls, cadaver, children, fetuses) are needed to understand the reason for the differences in the incidence of EACC shapes between the works. The other finding of this study was that the measured parameters including the disEACC–SC, EACC length, and angZR–EACC–SC were changing according to EACC shapes. In this context, we recommend that radiologic examination of EACC shapes is not to be ignored by surgeons in terms of patients' positioning, and the selection of appropriate surgical approach.

The average values of the parameters related to EACC in the literature are given in Table 8. The length (6.87 ± 0.86 mm) of EACC in the postpubescence period was smaller than that (7–7.5 mm) of Shaikh and Kulkarni's [18] study conducted on young dry skulls; while, EACC width (6.28 ± 0.83 mm) in the postpubescence period were greater than that (5.1–5.4 mm) of their data. They compared EACC diameter on fetal, adolescent (age range 13–25 years) and adult (age range > 25 years) dry skulls, and observed that EACC size progressively increased from intrauterine life to adult life, but its dimension did not change after 25 years [18]. The measurements related to EACC dimension in this study showed that the length and width of EACC did not change from the prepubescence period. In adult subjects, the mean data range of the length and width of EACC in the current literature was presented as 6.28–8.16 mm and 4.86–6.86 mm, respectively [1, 2, 5, 6, 14, 16, 18, 19, 21, 26], which showed that our findings belonging to the patients in the postpubescence period were compatible with the adult data range. Similar to Aoun et al. [2] and Shaikh and Kulkarni [18], males/females significant statistical difference was observed in terms of EACC dimension. Unlike the studies of Aoun et al. [2] (no left/right differences) and Naidoo et al. [14] (the longer left side compared to right side), we found that EACC length in right side was statistically longer than that in left side. On the other hand, EACC length on cases with oval shaped and tear-drop shaped was larger than that on cases with round shaped.

The mean values of the distance measurements in the literature are presented in Table 8 [2, 6, 16, 21, 26], which showed that our findings related to disEACC–SC (29.83 ± 3.05 mm) and disEACC–MSP (25.43 ± 1.98 mm) in the postpubescence period were compatible with the adult data range belonging to the disEACC–SC (28.60–31.36 mm) and disEACC–MSP (24.50–28.78 mm). We observed that the disEACC–MSP did not change from the prepubescence period; while, the disEACC–SC seemed to reach adult size in postpubescence period. In addition, the findings of this study showed that some distance measurements were changing according to EACC shapes (only the disEACC–SC) and sex (longer distance in males compared to females for the disEACC–MSP). The mean values of the angZR–EACC–SC (24.61 ± 4.72°) in the postpubescence period were smaller than the angle (36.59–37.11°) reported by Özalp et al. [16]. Some angles were changing according to EACC shapes (only the angZR–EACC–SC), sex (smaller angle in males compared to females for the angEAC–EACC–SC) and side (greater angle in right side compared to left side for the angEAC–EACC–SC, and smaller angle in right side compared to left side for the angZR–EACC–SC). Interestingly, we found that the angZR–EACC–SC was decreasing according to age between 1 and 20 years.

Table 7 The shape of EACC in the literature

Studies	Region	*N*	Techniques	Sample	Age	Oval shaped (%)	Round shaped (%)	Tear drop shaped (%)	Almond shaped (%)
Naidoo et al. [14]	South Africa	81	Anatomic	DS	Adult	49.4	28.4	22.2	–
Somesh et al. [21]	India	82	Anatomic	DS	Adult	30.67	52.14	–	17.17
Özalp et al. [16]	Turkey	20	Anatomic	DS	Adult	32.5	62.5	5	–
The current study	Turkey	200	CT scans	Patient	Child	58.3	24	17.8	–

N Number, *DS* Dry skulls, *CT* Computed tomography

Table 8 The size (e.g., length, width and surface area) and the distance from EACC to certain landmarks in the literature

Studies	*N*	Techniques	Sample	Age	Sex	Side	EACC length	EACC width	disEACC–MSP	disEACC–SC	angZR–EACC–SC
Ahmed et al. [1]	100	Anatomic	DS	Adult	–	Right	6.79 (5–8.5)	5.54 (4–7.5)	–	–	–
						Left	6.28 (5–8)	5.27 (4–7)	–	–	–
Naidoo et al. [14]	81	Anatomic	DS	14–100 y	–	–	5.41	7.52	–	–	–
Shaikh and Kulkarni [18]	235	Anatomic	DS	Fetus	–	Right	2.4 ± 1.2	1.8 ± 0.9	–	–	–
						Left	2.6 ± 1.3	1.8 ± 0.4	–	–	–
				Young (13–25y)	Male	Right	7.5 ± 1	5.3 ± 0.6	–	–	–
						Left	7.5 ± 1.2	5.4 ± 0.6	–	–	–
					Female	Right	7 ± 0.9	5.2 ± 0.9	–	–	–
						Left	7 ± 0.7	5.1 ± 0.6	–	–	–
				Adult (> 25 y)	Male	Right	7.6 ± 1.1	5.3 ± 0.8	–	–	–
						Left	7.5 ± 0.9	5.5 ± 0.8	–	–	–
					Female	Right	7.2 ± 1.1	5.3 ± 1.2	–	–	–
						Left	7.3 ± 1	5.3 ± 0.8	–	–	–
Aoun et al. [2]	150	Anatomic	DS	Adult	Male	Right	7.96 ± 0.89	5.7 ± 0.69	28.78 ± 2.15	31.1 ± 3.1	–
						Left	6.77 ± 0.8	5.58 ± 0.67	28.19 ± 1.97	30.9 ± 3.06	–
					Female	Right	7 ± 0.65	5 ± 0.5	26.4 ± 1.4	28.6 ± 2	–
						Left	6.77 ± 0.6	4.86 ± 0.44	25.99 ± 1.5	28.37 ± 1.99	–
Berlis et al. [5]	60	Anatomic	DS	Adult	–	–	7.81 ± 1.16	5.69 ± 0.35	–	–	–
		CT scans			–	–	7.91 ± 1.13	5.88 ± 0.64	–	–	–
Sharma and Garud [19]	50	Anatomic	DS	Adult	–	–	3.20–8.14	4.5–9.52	–	–	–
Somesh et al. [21]	82	Anatomic	DS	Adult	–	Right	8.13 ± 0.99	6.31 ± 0.64	25.42 ± 0.25	–	–
						Left	8.16 ± 1	6.19 ± 0.80	24.97 ± 0.25	–	–
Özalp et al. [16]	20	Anatomic	DS	Adult	–	–	8.02 ± 1.09	6.86 ± 0.90	25.95 ± 2.12	28.69 ± 2.84	37.11 ± 6.87
		CT scans					7.89 ± 1.14	6.41 ± 0.90	25.55 ± 2.13	28.71 ± 1.98	36.59 ± 4.94
Çalgüner et al. [6]	307	Anatomic	DS	Adult	Male	Right	–	–	25.63 ± 3.60	31.16 ± 2.62	–
						Left	–	–	25.67 ± 2.88	31.36 ± 2.87	–
					Female	Right	–	–	25.01 ± 3.59	29.77 ± 3.12	–
						Left	–	–	24.92 ± 2.45	31.13 ± 2.74	–
Zhong et al. [26]	120	CT scans	Patient	8–82 y	–	–	–	–	24.50 ± 1.26	–	–
The current study	200	CT scans	Patient	Child	–	–	6.41 ± 1.07	6.01 ± 0.87	23.80 ± 2.79	25.44 ± 4.44	27.72 ± 5.43

N Number, *DS* Dry skulls, *CT* Computed tomography, *y* years

Conclusion

Our findings suggested that EACC length, disEACC–MSP and EACC width did not change from the prepubescence period (between 10 and 13 years); while, the disEACC–SC seemed to reach adult size in postpubescence period (between 14 and 20 years). The measured parameters including the length, width, angle and distance to certain anatomical landmarks were changing according to EACC shapes, sexes and sides. In this context, we recommend that radiologic examination of EACC shape, location and size is not to be ignored by surgeons in terms of patients positioning, and the selection of appropriate surgical approach.

Author contributions BT, OB, YB, FÇ, HÖ, VH, DT, DÜT: project development, data collection, data analysis, manuscript writing, manuscript editing. MÇD, YV, CB: project development, data analysis, manuscript editing.

Funding This research did not receive any specific grant from funding agencies in the public, commercial, or not-for-profit sectors.

Compliance with ethical standards

Conflict of interest The authors declare no conflict of interest.

References

1. Ahmed MM, Jeelani M, Tarnum A (2015) Anthropometry: a comparative study of right and left sided foramen ovale, jugular foramen and carotid canal. Int J Sci Stud 3:88–94
2. Aoun MA, Nasr AY, Aziz AMA (2013) Morphometric study of the carotid canal. Life Sci J 10:2559–2562
3. Aslan A, Balyan FR, Taibah A, Sanna M (1998) Anatomic relationships between surgical landmarks in type b and type c infratemporal fossa approaches. Eur Arch Otorhinolaryngol 255:259–264
4. Babu RP, Sekhar LN, Wright DC (1994) Extreme lateral transcondylar approach: technical improvements and lessons learned. J Neurosurg 81:49–59
5. Berlis A, Putz R, Schumacher M (1992) Direct and CT measurements of canals and foramina of the skull base. Br J Radiol 65:653–661
6. Calgüner E, Turgut HB, Gözil R, Tunç E, Sevim A, Keskil S (1997) Measurements of the carotid canal in skulls from Anatolia. Acta Anat (Basel) 158:130–132
7. Cicekcibasi AE, Murshed KA, Ziylan T, Şeker M, Tuncer I (2004) A morphometric evaluation of some important bony landmarks on the skull base related to sexes. Turk J Med Sci 34:37–42
8. George B, DeMantos C, Cophignon J (1988) Lateral approach to the anterior portion of the foramen magnum. Surg Neurol 29:484–490
9. Gil Z, Constantini S, Spektor S et al (2005) Skull base approaches in the pediatric population. Head Neck 27:682–689
10. Gonzalez LF, Walker MT, Zabramski JM et al (2003) Distinction between paraclinoid and cavernous sinus aneurysms with computed tomographic angiography. Neurosurgery 52:1131–1137
11. Goodway JD, Ozmun JC, Gallahue DL (2019) Understanding motor development: infants, children, adolescents, adults. Jones & Bartlett Learning, Burlington
12. Goudihalli SR, Goto T, Bohoun C et al (2018) Sympathetic plexus schwannoma of carotid canal: two cases with surgical technique and review of literature. World Neurosurg 118:63–68
13. Kreiborg S, Björk A (1982) Description of a dry skull with crouzon syndrome. Scand J Plast Reconstr Surg 16:245–253
14. Naidoo N, Lazarus L, Ajayi NO, Satyapal KS (2017) An anatomical investigation of the carotid canal. Folia Morphol (Warsz) 76:289–294
15. Orakdöğen M, Berkman Z, Erşahin M, Biber N, Somay H (2007) Agenesis of the left internal carotid artery associated with anterior communicating artery aneurysm: case report. Turk Neurosurg 17:273–276
16. Özalp H, Beger O, Erdoğan O et al (2019) Morphometric assessment of the carotid foramen for lateral surgical approach. J Int Adv Otol 15:222–228
17. Resnick DK, Subach BR, Marion DW (1997) The significance of carotid canal involvement in basilar cranial fracture. Neurosurgery 40:1177–1181
18. Shaikh VG, Kulkarni PR (2014) A study of morphology, morphometry, symmetry and development of external opening of carotid canal with comparison in male, female and foetus. Int J Anat Res 2:797–805
19. Sharma NA, Garud RS (2011) Morphometric evaluation and a report on the aberrations of the foramina in the intermediate region of the human cranial base: a study of an Indian population. Eur J Anat 15:140–149
20. Shlomi B, Chaushu S, Gil Z, Chaushu G, Fliss DM (2007) Effects of the subcranial approach on facial growth and development. Otolaryngol Head Neck Surg 136:27–32
21. Somesh MS, Sridevi HB, Murlimanju BV, Pai SR (2014) Morphological and morphometric study of carotid canal in Indian population. Int J Biomechanical Res 5:455–460
22. Wasserzug O, DeRowe A, Ringel B et al (2018) Open approaches to the anterior skull base in children: review of the literature. J Neurol Surg B Skull Base 79:42–46
23. Watanabe A, Omata T, Koizumi H, Nakano S, Takeuchi N, Kinouchi H (2010) Bony carotid canal hypoplasia in patients with moyamoya disease. J Neurosurg Pediatr 5:591–594
24. Weninger WJ, Müller GB (1999) The parasellar region of human infants: cavernous sinus topography and surgical approaches. J Neurosurg 90:484–490
25. York G, Barboriak D, Petrella J, DeLong D, Provenzale JM (2005) Association of internal carotid artery injury with carotid canal fractures in patients with head trauma. AJR Am J Roentgenol 184:1672–1678
26. Zhong S, Ren J, Zhang Y et al (2018) Anatomic Study of Craniocervical Junction and Its Surrounding Structures in Endoscopic Transoral-Transpharyngeal Approach. J Craniofac Surg 29:1973–1977